

**Suppressed superconductivity in charge-doped Li(Fe<sub>1-x</sub>Co<sub>x</sub>)As single crystals**

S. Aswartham,<sup>1</sup> G. Behr,<sup>1</sup> L. Harnagea,<sup>1</sup> D. Bombor,<sup>1</sup> A. Bachmann,<sup>1</sup> I. V. Morozov,<sup>1,2</sup> V. B. Zabolotnyy,<sup>1</sup>  
 A. A. Kordyuk,<sup>1</sup> T. K. Kim,<sup>1</sup> D. V. Evtushinsky,<sup>1</sup> S. V. Borisenko,<sup>1</sup> A. U. B. Wolter,<sup>1</sup> C. Hess,<sup>1</sup>  
 S. Wurmehl,<sup>1,\*</sup> and B. Büchner<sup>1</sup>

<sup>1</sup>Leibniz Institute for Solid State and Materials Research, D-01069 Dresden, Germany

<sup>2</sup>Department of Chemistry, Moscow State University, Moscow 119991, Russia

(Received 6 May 2011; revised manuscript received 22 July 2011; published 12 August 2011)

Single crystals of the new unconventional superconductor LiFe<sub>1-x</sub>Co<sub>x</sub>As with  $x = 0, 0.025, 0.05$  were grown by a new approach using the self-flux technique. The superconducting transition temperature was found to decrease upon Co doping at the Fe site. Apparently, in LiFeAs this doping scheme suppresses superconductivity, in contrast to the effects of Co doping in other Fe-As compounds, where it suppresses the spin-density wave and establishes superconductivity. Angle-resolved photoemission spectroscopy shows that the bottom of electron-like bands sinks by about 17 meV upon 5% Co doping, which indicates that the chemical substitution of Co for Fe in LiFeAs results in charge doping.

DOI: [10.1103/PhysRevB.84.054534](https://doi.org/10.1103/PhysRevB.84.054534)

PACS number(s): 74.25.Jb, 74.62.Bf, 74.70.Xa

**I. INTRODUCTION**

In the field of superconductivity, LiFeAs has recently generated enormous interest among the researchers working with Fe-based superconductors.<sup>1</sup> Interestingly, one of the first publications on LiFeAs dates back to 1968,<sup>2</sup> though it did not attract much interest until the recent discovery of superconductivity in Fe-As compounds.<sup>3</sup> Among different types of Fe-based superconductors, LiFeAs has been found to be a unique representative. One reason is that the magnetically ordered spin-density wave state, which is suppressed upon doping and is considered to be obligatory for superconductivity in all Fe-As superconductors,<sup>4-6</sup> is not present in LiFeAs even after the application of pressure up to 20 GPa.<sup>7</sup>

Since the occurrence of a spin-density wave is closely connected to the form of the Fermi surface, a detailed study of the electronic structure has been performed to clarify this issue. Recent angle-resolved photoemission spectroscopy (ARPES) investigations on LiFeAs reveal the absence of Fermi surface nesting, high renormalization of the conduction bands, and high density of states at the Fermi level.<sup>8</sup> This brings up the question of how superconductivity is derived in the stoichiometric superconductor LiFeAs. Recent studies on this system have speculated that LiFeAs could be a triplet  $p$ -wave superconductor,<sup>9,10</sup> although precise determination and further investigations are necessary to confirm this. This emphasizes the importance of further experimental and theoretical studies of the LiFeAs system.

Owing to the complexities involved in the synthesis, such as the sample handling, LiFeAs turns out to be one of the least studied iron arsenides, especially when compared to the 122 family. The parent compound LiFeAs crystallizes in a tetragonal Cu<sub>2</sub>Sb/PbClF-type structure ( $P4/nmm$ ) and consists of Fe<sub>2</sub>As<sub>2</sub> layers connected by edge-sharing FeAs<sub>4</sub> tetrahedra, similar to other pnictide superconductors.<sup>11</sup> It is well known that all Fe-based superconductors are quite sensitive to chemical substitution and pressure. Even in the isostructural NaFeAs, chemical substitution has been shown to affect  $T_C$  significantly.<sup>12</sup> This generated interest toward chemical substitution in the stoichiometric, isostructural, and isovalent superconductor LiFeAs. In particular, Pitcher *et al.*<sup>13</sup>

have recently reported on the substitution of Fe by Co and Ni in polycrystalline LiFeAs samples. Here, extending the previous work, we report on the growth of LiFe<sub>1-x</sub>Co<sub>x</sub>As ( $x = 0.025$  and  $0.05$ ) single crystals, their magnetic and transport properties, and their electronic structure studied by ARPES.

**II. MATERIALS AND METHODS**

Single crystals of LiFe<sub>1-x</sub>Co<sub>x</sub>As with  $x = 0.025, 0.05$  were grown by a self-flux technique; for details, see Ref. 14. All preparation steps have been performed in an argon-filled glove box with O<sub>2</sub> and H<sub>2</sub>O content less than 0.1 ppm. For the 2.5% Co-doped sample, powder materials of Fe (Alfa Aesar, 99.99%) and As (Alfa Aesar, 99.99%), lumps of Li (Alfa Aesar, 99.9%), and Co powder (Alfa Aesar, 99.98%) were used. Initially, As, Fe, and Co were ground thoroughly in an agate mortar to ensure homogeneity, and then small lumps of the Li metal were added to the Fe-Co-As mixture. A molar ratio of Li:Fe<sub>1-x</sub>Co<sub>x</sub>:As = 3:2:3 was used. For the 5% Co-doped sample we used prereacted FeAs, Co<sub>2</sub>As, and metallic Li lumps in the molar ratio of 3:2:3. For each growth, in total 5 g of the precursor material were taken in a niobium crucible and welded under 1.2 atmospheric pressure of Ar in an arc-melting facility. The niobium crucible assembly was heated up to 1363 K for 18 h, kept at this point for 5 h, and cooled down to 873 K at a rate of 4.5 K/h. Thin millimeter-sized plate-like single crystals were extracted mechanically from the ingot. The inset of Fig. 1(b) exemplarily shows an as-grown LiFe<sub>0.95</sub>Co<sub>0.05</sub>As single crystal. All crystals grow in a layered morphology with a thickness of the order of micrometers; they are easy to cleave along the  $ab$  plane. The layered morphology is apparent in the electron microscope picture [Fig. 1(a)]. Single crystals of two doping levels, i.e., LiFe<sub>1-x</sub>Co<sub>x</sub>As with  $x = 0.025, 0.05$ , were grown using this method. All LiFe<sub>1-x</sub>Co<sub>x</sub>As single crystals are fragile, are prone to exfoliation, and are even more sensitive to air moisture compared to LiFeAs single crystals.

The quality of the as-grown single crystals was assessed by several complementary techniques. Several samples were examined with a scanning electron microscope (SEM, XL30

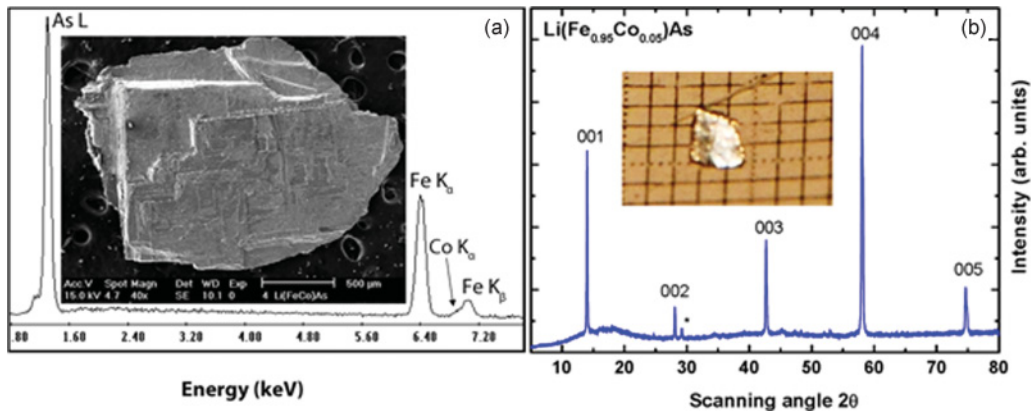


FIG. 1. (Color online) (a) EDX spectrum of a  $\text{LiFe}_{0.95}\text{Co}_{0.05}\text{As}$  single crystal. The inset shows a SEM picture. (b) XRD pattern of a  $\text{LiFe}_{0.95}\text{Co}_{0.05}\text{As}$  single crystal. The inset exemplarily shows the picture of an as-grown  $\text{LiFe}_{0.95}\text{Co}_{0.05}\text{As}$  single crystal with a shiny and metallic-like surface.

Philips, IN400) equipped with an electron microprobe analyzer for semiquantitative elemental analysis using the energy dispersive x-ray (EDX) mode. Figure 1(a) shows a SEM picture of a  $\text{LiFe}_{0.95}\text{Co}_{0.05}\text{As}$  single crystal. The composition is determined by averaging over several points of the same specimen and for several crystals of each batch. Figure 1(a) exemplarily shows such a typical EDX spectrum. The shoulder close to the  $\text{Fe-K}_\beta$  line at 7 keV clearly confirms the presence of Co and gives a relatively good estimate of the Co composition. The average Co concentrations, measured by EDX for  $x_{\text{nominal}} = 2.5\%$ ,  $5\%$ , are  $x_{\text{EDX}} = 3.6\%$ ,  $5.6\%$ . Thus, the deviations from the nominal values are within the absolute error limits of the EDX method. However, the slightly enhanced values as determined from EDX indicate a trend of the actual Co concentrations to be somewhat higher than the nominal ones. A possible explanation might be excess Co that has been taken from the flux during the growth of these crystals. Phase purity of the grown crystals was checked using x-ray diffraction. In order to avoid the degradation of the crystal in air, it was immersed in Fomblin oil. Figure 1(b) shows a diffraction pattern taken on a plate-like single crystal using a Rigaku miniflex with  $\text{Cu-K}_\alpha$  radiation. The reflections are indexed to  $00l$ , indicating the  $c$ -axis orientation. However, we see an additional reflection, marked by an asterisk, which might indicate that the crystal already started to decompose.

The magnetization was measured in a Quantum Design superconducting quantum interference device (SQUID) magnetometer, and all necessary care was taken to avoid exposing the sample to air, in particular during the time needed for mounting the sample in the magnetometer. All the magnetization measurements were performed after cooling the sample in zero magnetic field from far above the critical temperature. In-plane resistivity of several crystals was measured using a standard four-probe alternating current dc technique. The electrical contacts were attached in an argon-filled glove box using a two-component silver-filled epoxy and were cured at  $100^\circ\text{C}$  in vacuum. For mounting the samples in our home-built measurement system were covered with Apiezon N high-vacuum grease, which provides protection from air for some hours. Photoemission experiments for this study have been carried out using synchrotron radiation from the BESSY storage ring at the “1-cubed ARPES” station equipped

with a  $^3\text{He}$  cryostat. The single crystals were mounted on the sample holders in Ar atmosphere and afterward placed in Ar-filled ampoules. The Ar atmosphere was only broken for a short moment, just before introducing the samples into the ultrahigh vacuum chamber (UHV). Each so-prepared sample was cleaved directly in the UHV, and it was ensured that the samples exhibited a mirror-like surface before the spectra were recorded. The excitation energy was set to 70 and 50 eV for the pure and Co-doped samples, respectively. Effective energy and momentum resolution were set to 10 meV and  $0.5^\circ$ , respectively. The data presented in this paper were measured using horizontally polarized light with a beam-spot size of about  $100 \times 50 \mu\text{m}^2$ . Such a beam-spot size results in averaging of all possible nanoscale inhomogeneities, and the ARPES spectra yield the averaged electronic structures for both the pure and substituted samples. Importantly, the ARPES experiment did not reveal any changes in the spectra when moving the beam spot over the sample surface (1–2 mm rambling range), further confirming the high quality of our crystals. More information about the experimental geometry can be found elsewhere.<sup>15</sup>

### III. RESULTS AND DISCUSSION

#### A. Magnetic measurements

Figure 2 presents the temperature dependence of the volume susceptibility ( $4\pi\chi_V$ ).  $\chi_V$  has been deduced from the measured magnetization by correcting for demagnetization effects using an ellipsoidal approximation.<sup>16</sup> We determine  $T_C$  from the bifurcation point between zero-field-cooled (zfc) and field-cooled (fc) magnetization, and it is found to be 16.8, 13.8, and 10.8 K for  $x = 0, 2.5\%$ , and  $5\%$ , respectively. Interestingly, the substitution of Fe by small amounts of Co apparently results in a significant decrease of the superconducting transition temperature, unlike in the isostructural  $\text{NaFeAs}$ , where a strong interplay between antiferromagnetism and superconductivity occurs upon doping with Co and Ni and where superconductivity appears to be stabilized by the substitutions.<sup>12</sup> However, despite the suppression of superconductivity, no signatures of structural or magnetic transitions are observed in the Co-doped samples. These observations are unexpected, as,

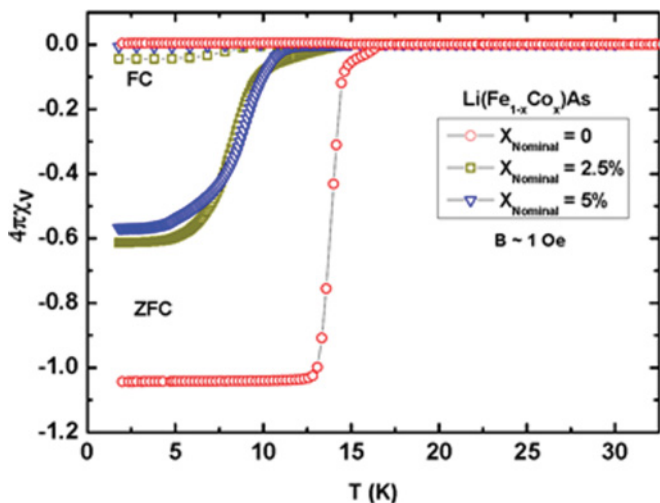


FIG. 2. (Color online) (a) Temperature dependence of the volume susceptibility ( $4\pi\chi_V$ ) of  $\text{LiFe}_{0.95}\text{Co}_{0.025}\text{As}$  (green squares) and of  $\text{LiFe}_{0.95}\text{Co}_{0.05}\text{As}$  (blue triangles) with zero-field cooling (zfc) and field cooling (fc) in  $B = 1$  Oe. All data have been collected for  $B \parallel ab$ .

e.g., doping with charge carriers in the  $\text{BaFe}_2\text{As}_2$  suppresses the spin-density wave and introduces superconductivity.<sup>17,18</sup> However, in the present case, superconductivity is suppressed by introducing charge carriers in the  $\text{LiFeAs}$  system. As we can see in Fig. 2, not only does the superconducting transition temperature get suppressed upon Co doping, but the width of the transition becomes broader and the superconducting volume fraction decreases compared to the sharp transition and 100% volume fraction observed for the undoped  $\text{LiFeAs}$ . This is in agreement with the recent observation of Pitcher *et al.*, who also observed a decrease of  $T_C$ , a broadening of the superconducting transition, and a decrease of the volume fraction upon Co doping in polycrystalline samples of  $\text{LiFe}_{1-x}\text{Co}_x\text{As}$ .<sup>13</sup> Summarizing the reports in the literature about the  $\text{LiFeAs}$  system, the decrease in  $T_C$  and the decrease of the superconducting volume fraction seem to be a general result upon doping of charge carriers and/or the presence of impurities in the  $\text{LiFeAs}$  system,<sup>11,13,19</sup> which is in line with our results.

### B. Electrical resistivity

For each doping level several samples were studied, which yielded a reproducible normalized resistivity (see Fig. 3). However, we observed an unusual spread in their absolute values, clearly exceeding the usual error of the geometric factor ( $\leq 10\%$ ). The reason for this variation is presently unclear. Nevertheless, the resistivity at room temperature can be specified to be in the range of 0.3–0.6 m $\Omega$  cm.

We observe several systematic tendencies with increasing Co doping. The residual resistivity ratio  $\rho(300\text{K})/\rho(20\text{K})$  decreases from 24 ( $x = 0$ ) to 7 ( $x = 5\%$ ). This is consistent with a doping-enhanced residual resistivity, which is caused by enhanced scattering off Co dopants. The superconducting transition width is broadened, and it is shifted to lower temperatures. Using the 90/10 criterion, typical superconducting transitions are at  $T_c = (16.6 \pm 0.7)$  K for

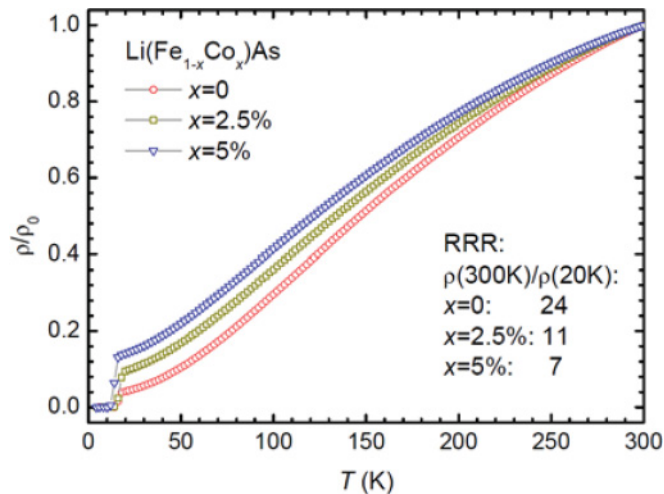


FIG. 3. (Color online) Temperature dependence of the electrical resistivity  $\parallel ab$  for different Co-doping levels  $x$  of  $\text{LiFe}_{1-x}\text{Co}_x\text{As}$ , normalized to the room-temperature value.

the undoped compound and  $T_c^{2.5\%} = (16.6 \pm 1.1)$  K and  $T_c^{5\%} = (14.0 \pm 1.2)$  K for the 2.5% and 5% doped samples, respectively. Note that, using this criterion for determining  $T_c$ , the downgraded superconducting properties at  $x = 0.025$  are essentially reflected in the broadened transition width. A more suitable criterion, which also is in line with the results from magnetic susceptibility, is the onset temperature of zero resistance. The corresponding values are  $T_{c,\text{zero}}^{0\%} = 15.6$  K,  $T_{c,\text{zero}}^{2.5\%} = 13.4$  K, and  $T_{c,\text{zero}}^{5\%} = 11.2$  K, which differ by no more than 1 K from susceptibility measurements.

### C. ARPES

In a recent density functional theory (DFT) calculation, it was suggested that substitution of Fe by Co in iron arsenides should not dope carriers but should remain rather isovalent to Fe.<sup>20</sup> Therefore, it is very interesting and important to check how this prediction compares with experimental data. Though the electronic structure of the 122 family of iron arsenides can be studied with relative ease through photoemission,<sup>21</sup> recent combined scanning tunneling microscopy and low-energy electron diffraction<sup>22</sup> as well as a combined study of low-energy electron diffraction with ARPES<sup>23</sup> indicate that a cleaved surface of Co-doped  $\text{Ba}(\text{Fe}_{1-x}\text{Co}_x)_2\text{As}_2$  exhibits a complex diversity of ordered and disordered structures, which may result in altered electronic structure at the surface. In this regard,  $\text{LiFeAs}$  appears to be much better suited to study the effect of Co substitution. Additional advantages are the absence of surface states<sup>24</sup> and the general agreement between the electronic structure observed in ARPES experiments and local-density approximation (LDA) calculations.<sup>8</sup>

As follows from the Luttinger theorem,<sup>25</sup> the volume of the Fermi surface (FS) determines the total amount of doped charge and is frequently used when analyzing ARPES spectra of layered compounds.<sup>26</sup> However, in the present case, the determination of the FS volume would require “mapping” of the full  $k_z$  dispersion due to the notable  $k_z$  dispersion on the electron-like Fermi surface sheets. A more reliable and at the same time easier way is to compare the depth of the electron

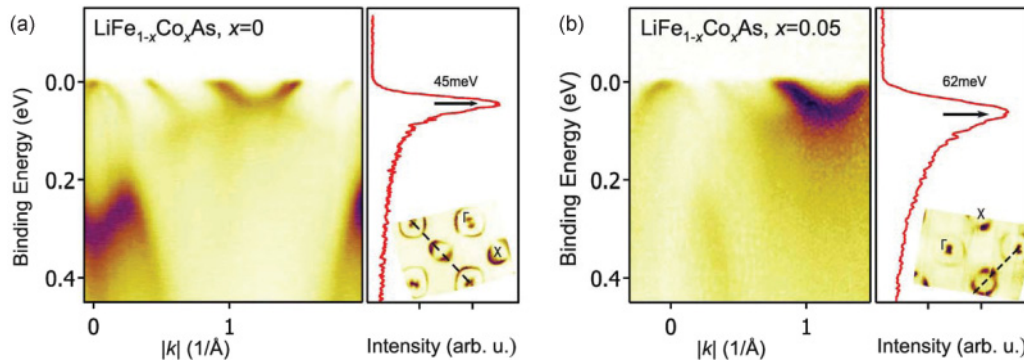


FIG. 4. (Color online) Energy momentum cuts representing ARPES intensity along the  $\Gamma$ - $X$ - $\Gamma$  direction for the (a) pure and (b) 5% doped LiFeAs. The cut positions in the reciprocal space are shown by dashed lines superimposed on the experimental Fermi surface maps shown as insets. The red curves to the right of the cuts are energy distribution curves (EDCs) taken at the  $X$  point, with arrows denoting the energy position for the bottom of the electron pocket.

bands at the  $X$  point, which is expected to increase upon electron doping. Also favorable is the fact that, according to the band structure calculations, this parameter has a negligible  $k_z$  dispersion,<sup>24,27</sup> so that different  $k_z$  would not be a problem here.

Figures 4(a) and 4(b) contain the experimental energy-momentum intensity distribution for the pure and 5% Co-substituted LiFeAs, which were measured along the  $\Gamma$ - $X$ - $\Gamma$  direction, as shown in the insets. In Fig. 4 the dark color represents high intensity, generally following band dispersion. For a better determination of the band bottom each panel contains an  $X$ -point energy dispersion curve, which simply represents the photointensity at that  $k$  point. As one may see from Fig. 4, for the 5%-doped LiFeAs the bottom position of the electron band is found to be  $\sim 17$  meV lower in energy, as compared to the undoped compound, which, indeed, corresponds to electron doping. Moreover, while the ARPES spectrum of the pure LiFeAs is rather sharp, the spectrum significantly broadens upon the substitution of Fe by Co. This broadening might indicate that, apart from the charge doping, the substitution of Fe by Co also leads to disorder. This interpretation is consistent with the results of the electrical transport as discussed in Sec. III B, where the increase of the residual resistivity with the concomitant decrease of the residual resistivity ratio with increasing Co content may also be attributed to enhanced scattering due to disorder.

Here one may become a bit semiquantitative. Assuming a rigid band shift and band renormalization with a factor of 3<sup>8</sup>, we have estimated the change to the 3D Fermi surface volume using the LDA band structure presented in Ref. 8. The difference in the Fermi surface volume in this case corresponds to a doping close to 0.09 electrons per Fe atom. Obviously, a rigid band shift and an equal renormalization factor for

all bands that are crossing the Fermi level are rather crude assumptions, though sufficient enough to establish the fact that Co substitution in LiFeAs result in a charge doping comparable to the chemical substitution level.

#### IV. SUMMARY AND CONCLUSION

In summary, single crystals of the new unconventional superconductor LiFe<sub>1-x</sub>Co<sub>x</sub>As with  $x = 0.025, 0.05$  were grown. We characterized the crystals with SEM EDX, and the superconducting properties have been studied by means of temperature-dependent electrical resistivity and magnetic-susceptibility measurements. While the parent compound exhibits a sharp superconducting transition, doping with Co at the Fe site suppresses superconductivity quite rapidly. The electronic structure has been studied by ARPES, which confirms electron doping upon the substitution of Fe by Co. This study confirms that LiFeAs is unique among the Fe-based superconductors, as charge doping in, e.g., the 122 family suppresses the spin-density wave and introduces superconductivity.

#### ACKNOWLEDGMENTS

The authors thank M. Deuschmann, S. Pichl, and S. Gass for technical support. Work has been supported by the DFG through the Priority Programme SPP1458 (Grants No. BE1749/13 and No. GR3330/2). I.M. acknowledges support from the Ministry of Science and Education of the Russian Federation under State Contract No. P-279 and by RFBR-DFG (Project No. 10-03-91334).

\*s.wurmehl@ifw-dresden.de

<sup>1</sup>J. H. Tapp, Z. Tang, B. Lv, K. Sasmal, B. Lorenz, P. C. W. Chu, and A. M. Guloy, *Phys. Rev. B* **78**, 060505 (2008).

<sup>2</sup>R. Juza and K. Z. Langer, *Z. Anorg. Allg. Chem.*, **58**, 361 (1968).

<sup>3</sup>Y. Kamihara, T. Watanabe, M. Hirano, and H. Hosono, *J. Am. Chem. Soc.* **130**, 3296 (2008).

<sup>4</sup>H. Luetkens, H.-H. Klauss, M. Kraken, F. J. Litterst, T. Dellmann, R. Klingeler, C. Hess, R. Khasanov, A. Amato, C. Baines,

M. Kosmala, O. J. Schumann, M. Braden, J. Hamann-Borrero, N. Leps, A. Kondrat, G. Behr, J. Werner, and B. Büchner, *Nat. Mater.* **8**, 305 (2009).

<sup>5</sup>A. J. Drew, Ch. Niedermayer, P. J. Baker, F. L. Pratt, S. J. Blundell, T. Lancaster, R. H. Liu, G. Wu, X. H. Chen, I. Watanabe, V. K. Malik, A. Dubroka, M. Rössle, K. W. Kim, C. Baines, and C. Bernhard, *Nat. Mater.* **8**, 310 (2009).

- <sup>6</sup>J.-H. Chu, J. G. Analytis, C. Kucharczyk, and I. R. Fisher, *Phys. Rev. B* **79**, 014506 (2009).
- <sup>7</sup>S. J. Zhang, X. C. Wang, R. Sammynaiken, J. S. Tse, L. X. Yang, Z. Li, Q. Q. Liu, S. Desgreniers, Y. Yao, H. Z. Liu, and C. Q. Jin, *Phys. Rev. B* **80**, 014506 (2009).
- <sup>8</sup>S. V. Borisenko, V. B. Zabolotnyy, D. V. Evtushinsky, T. K. Kim, I. V. Morozov, A. N. Yaresko, A. A. Kordyuk, G. Behr, A. Vasiliev, R. Follath, and B. Büchner, *Phys. Rev. Lett.* **105**, 067002 (2010).
- <sup>9</sup>P. M. R. Brydon, M. Daghofer, C. Timm, and J. van den Brink, *Phys. Rev. B* **83**, 060501 (2011).
- <sup>10</sup>S.-H. Baek, H.-J. Grafe, F. Hammerath, M. Fuchs, L. Harnagea, S. Wurmehl, J. van den Brink, and B. Büchner (unpublished).
- <sup>11</sup>M. J. Pitcher, D. R. Parker, A. Paul, Sebastian J. C. Herkelrath, A. T. Boothroyd, R. M. Ibberson, M. Brunelli, and S. J. Clarke, *Chem. Commun* **45**, 5918 (2008).
- <sup>12</sup>D. R. Parker, M. J. P. Smith, T. Lancaster, A. J. Steele, I. Franke, P. J. Baker, F. L. Pratt, M. J. Pitcher, S. J. Blundell, and S. J. Clarke, *Phys. Rev. Lett.* **104**, 057007 (2010).
- <sup>13</sup>M. J. Pitcher, T. Lancaster, J. D. Wright, I. Franke, A. J. Steele, P. J. Baker, F. L. Pratt, W. T. Thomas, D. R. Parker, S. J. Blundell, and S. J. Clarke, *J. Am. Chem. Soc.* **132**, 10467 (2010).
- <sup>14</sup>I. Morozov, A. Boltalin, O. Volkova, A. Vasiliev, O. Kataeva, U. Stockert, M. Abdel-Hafiez, D. Bombor, A. Bachmann, L. Harnagea, M. Fuchs, H.-J. Grafe, G. Behr, R. Klingeler, S. V. Borisenko, C. Hess, S. Wurmehl, and B. Büchner, *Cryst. Growth Design* **10**, 4428 (2010).
- <sup>15</sup>V. B. Zabolotnyy, S. V. Borisenko, A. A. Kordyuk, D. S. Inosov, A. Koitzsch, J. Geck, J. Fink, M. Knupfer, B. Büchner, S. L. Drechsler, V. Hinkov, B. Keimer, and L. Patthey, *Phys. Rev. B* **76**, 024502 (2007).
- <sup>16</sup>J. A. Osborne, *Phys. Rev.* **67**, 351 (1945).
- <sup>17</sup>M. Rotter, M. Tegel, and D. Johrendt, *Phys. Rev. Lett.* **101**, 107006 (2008).
- <sup>18</sup>A. S. Sefat, R. Jin, M. A. McGuire, B. C. Sales, D. J. Singh, and D. Mandrus, *Phys. Rev. Lett.* **101**, 117004 (2008).
- <sup>19</sup>F. L. Pratt, P. J. Baker, S. J. Blundell, T. Lancaster, H. J. Lewtas, P. Adamson, M. J. Pitcher, D. R. Parker, and S. J. Clarke, *Phys. Rev. B* **79**, 052508 (2009).
- <sup>20</sup>H. Wadati, I. Elfimov, and G. A. Sawatzky, *Phys. Rev. Lett.* **105**, 157004 (2010).
- <sup>21</sup>V. B. Zabolotnyy, D. V. Evtushinsky, A. A. Kordyuk, D. S. Inosov, A. Koitzsch, A. V. Boris, G. L. Sun, C. T. Lin, M. Knupfer, and B. Büchner, *Phys. C* **469**, 448 (2009).
- <sup>22</sup>F. Massee, S. de Jong, Y. Huang, J. Kaas, E. van Heumen, J. B. Goedkoop, and M. S. Golden, *Phys. Rev. B* **80**, 140507 (2009).
- <sup>23</sup>E. van Heumen, J. Vuorinen, K. Koepernik, F. Massee, Y. Huang, M. Shi, J. Klei, J. Goedkoop, M. Lindroos, J. van den Brink, and M. S. Golden, *Phys. Rev. Lett.* **106**, 027002 (2011).
- <sup>24</sup>A. Lankau, K. Koepernik, S. Borisenko, V. Zabolotnyy, B. Büchner, J. van den Brink, and H. Eschrig, *Phys. Rev. B* **82**, 184518 (2010).
- <sup>25</sup>J. M. Luttinger, *Phys. Rev.* **119**, 1153 (1960).
- <sup>26</sup>S. V. Borisenko, M. S. Golden, S. Legner, T. Pichler, C. Dürr, M. Knupfer, J. Fink, G. Yang, S. Abell, and H. Berger, *Phys. Rev. Lett.* **84**, 4453 (2000).
- <sup>27</sup>I. A. Nekrasov, Z. V. Pchelkina, and M. V. Sadovskii, *JETP Lett.* **88**, 543 (2008).